2-1-1989

Convective Regimes in reactive Fluid media due to the interaction with Catalytic Surfaces

Hendrik J. Viljoen
University of Nebraska-Lincoln, hviljoen1@unl.edu

Jorge E. Gatica
State University of New York at Buffalo

Vladimir Hlavacek
State university of New York at Buffalo

Convective regimes in reactive fluid media due to the interaction with catalytic surfaces

Hendrik J. Viljoen, Jorge E. Gatica, and Vladimir Hlavacek

Citation: Physics of Fluids A: Fluid Dynamics **1**, 274 (1989); doi: 10.1063/1.857443
View online: https://doi.org/10.1063/1.857443
View Table of Contents: http://aip.scitation.org/toc/pfa/1/2
Published by the American Institute of Physics

Convective regimes in reactive fluid media due to the interaction with catalytic surfaces

Hendrik J. Viljoen[a)]
Centre for Advanced Computing and Decision Support, P.O. Box 395, Pretoria 0001, South Africa
Jorge E. Gatica and Vladimir Hlavacek
Department of Chemical Engineering, State University of New York at Buffalo, Amherst, New York 14260

(Received 29 September 1987; accepted 7 September 1988)

Reactive fluid media enclosed in a cavity with a catalytic surface are analyzed. Nonisothermal chemical reactions on this surface can lead to convective instabilities. A simplified model is developed by using a low-order truncation of a Fourier-type expansion and employing the Galerkin method. A linear stability analysis is presented and it is shown that, under certain conditions, the marginal curve for the onset of oscillatory instabilities can lie below that for monotonic ones. The stability of the convective modes is studied by nonlinear stability analysis and it is shown how they can evolve into periodic and nonperiodic motion patterns. Numerical results are provided to support and confirm analytical predictions.

I. INTRODUCTION

The Rayleigh–Bénard problem has been the subject of study and analysis by a large number of scientists. This is perhaps a result of the fact that this problem can display many important features of convective instabilities in fluid media. For instance, the characteristics of the boundaries will strongly influence the stability of a motionless basic state. Thus the effect of rigid side walls will allow only specific wavenumber perturbations to survive. For certain aspects ratios, competition between a pair of modes will be observed at the onset of convection.[1] The principle of exchange of stabilities does not always hold for deformable boundaries,[2] and three-dimensional rigid enclosures prevent truly two-dimensional convective structures.[3]

In reactive fluid media the chemical reaction can provide the driving force for convection and a similar problem to that of Bénard originates. The problem of convective instabilities due to the existence of a chemical reaction has already been reported in the literature. Bdzil and Frisch[5] considered a reversible exothermic reaction in a homogeneous fluid. The horizontal planes were kept at constant temperature and concentration, and the Bénard problem was recovered at chemical equilibrium. When the chemical equilibrium was disturbed the reaction rate was approximated by a first-order Taylor expansion and, by using the Galerkin method, a set of spectral equations was derived. A nonlinear analysis was performed by considering the interaction of different modes in the convective term. Gitterman and Steinberg[4] carried out a linear stability analysis for binary mixtures with chemical reaction. These authors reported on the possibility of monotonic or oscillatory instabilities at the first bifurcation point.

If the chemical reaction occurs as a result of interaction between reactive fluids and catalytic surfaces, the reaction is said to be heterogeneous. When a nonisothermal reaction takes place at the catalytic surface, the heat generated (consumed) by an exothermic (endothermic) reaction as well as the difference in molecular weight (or phase) between reactants and products will determine density gradients. Depending on the location of the catalytic wall this gradient will have a definite orientation with respect to the gravitational field. This eventually may give rise to buoyancy forces which by overcoming the viscous damping can destabilize a motionless basic state.

The rate of reaction on a catalytic surface is determined by the relationship between the chemical kinetics of the reaction and the transport of reactants to the surface. For this reason, several authors studied the interaction between surface chemical reactions and natural convection. Gray and Kostin[6,7] studied a two-dimensional cavity with catalytic side walls. The reaction was exothermic and natural convection was only driven by the thermal expansion of the fluid. Semianalytical solutions of the temperature and flow fields were constructed and compared with numerical results. For this configuration, natural convection is stable for $\mathrm{Ra}_1 > 0$ (thermal Rayleigh number) and $\mathrm{Ra}_2 = 0$ (i.e., the density does not depend on the concentration). Pribytkova and Shtessel[8] studied an infinite horizontal layer with an inert bottom and a catalytic top. Natural convection is driven by the difference in density between reactants and products. A linear stability analysis of the basic state was performed. The eigenvalue problem was solved by approximating the eigenfunction by a Chebyshev polynomial, and a dispersion relation $\mathrm{Ra}_2(k)$ was derived. Pribytkova *et al.*[9] also considered an infinite horizontal layer, but they took both Rayleigh numbers, thermal and mass, into consideration. The dispersion relation reported, however, only holds for monotonic instabilities. These authors pointed out the differences in the critical values when the reaction operated either in the kinetic or diffusion regime. A similar problem was analyzed by Wankat and Schowalter; a linear stability analysis was performed and conditions for the onset of stationary instabilities reported.[10] Later these authors extended their previous

[a)] Current address: Department of Chemical Engineering, University of Stellenbosch, Stellenbosch 7600, South Africa.

 0899-8213/89/020274-11$01.90

work and used the Galerkin method to study the importance of oscillatory instabilities.[11]

Both Rayleigh numbers were also taken into account in the experimental study reported by Chefanov and Shtessel.[12] These authors studied the oxidation of sulfur dioxide on a platinum catalyst. Correlations between natural convection and enhancement of the heat transfer were given for a broad range of the system parameters.

In this study the authors want to emphasize the role of the free convection and the effect that the chemical reaction has on flow phenomena. It is worth noting that, in deposition reactions for instance, flow phenomena can have a great influence on surface morphology. Thus it is important to recognize the factors that can cause secondary flows, and to determine under what conditions these flows will be absent. It is precisely from this point of view that the analysis is presented.

The partial differential equations that describe the heat, mass, and momentum balances are not amenable to analysis and, even under mild conditions, they prove to be difficult to solve numerically. Therefore, it would be advantageous to make realistic simplifications that would cast these equations in a more tractable formulation. One way to simplify the equations is to use separation of variables and, by choosing appropriate trial functions, approximate the partial differential equations by a set of ordinary differential equations. These equations can then be easily integrated and a qualitative picture of the bifurcation behavior of the original system can be drawn. However, there are several shortcomings with this approach. In the study of the Bénard convection problem for a homogeneous fluid between two infinite horizontal planes, the horizontal spatial variables were approximated by the Fourier series. This is valid since the influence of the lateral walls is absent, and periodicity can be expected. The problem now arises of where to truncate the Fourier series. Lorenz[13] did a one-mode truncation of the vorticity equation and kept two modes for the temperature. It is well known that this initial value problem in R^3 gives chaotic behavior. Curry[14] showed that an expanded version (R^{14}) indeed shows different dynamic behavior. Foias *et al.*[15] proved that a finite-dimensional space of the same order as the thermal Rayleigh number will give a correct picture of solutions imbedded in an appropriate Banach space. This bound on truncation, however, is far too high to use existing continuation packages and still keep an advantage over a numerical scheme that solves the original problem.

If the horizontal layer is bounded by lateral walls, the boundary conditions for the velocities become different and the Fourier series cannot be used. Platten and Legros[16] and Luijkx and Platten[17] used Chebyshev polynomials to approximate the velocity in the horizontal variables. When a finite cavity is considered, truncation becomes valid since only a finite number of different convection modes will survive in this bounded domain.[18] However, a new problem arises. If the cavity is large enough to stabilize more than one mode, odd modes as well as even modes are no longer orthogonal with respect to the weight function 1 (or any other except $(1-x^2)^{-1/2}$, $x\in[-1,1]$ for that matter). This fact complicates the truncation point.

For the Rayleigh–Darcy problem (the analogous problem to Bénard in porous media) the analysis is simpler. For both infinite and finite cavities, the Fourier series satisfy the boundary conditions and, since they are orthogonal (for weight function 1, $x\in[-1,1]$), truncation becomes simpler. Viljoen and Hlavacek[19] studied chemically driven convection in a porous medium and employed this method to derive the spectral equations that were in good agreement with the numerical solution of the original problem.

The problem posed in this work will be treated in a similar fashion. First, it will be shown how the choice of the trial functions requires a careful analysis of the basic state. Furthermore, the requirement of meeting both (the nonslip and nonpenetration) boundary conditions on rigid walls adds another degree of complexity to the selection of the eigenfunctions. A linear stability analysis will be presented and conditions for the onset of convective instabilities will be reported. Second, the convective modes born at the onset of convection will be followed through nonlinear stability analysis and it will be shown how the system evolves in the parameter space losing the characteristic of periodicity. Finally, the numerical solution of the governing equations will be presented. By comparison between numerical results and analytical predictions, the power of the approach will be validated.

II. MODEL FORMULATION

It is the purpose of this work to analyze the situation where density gradients resulting from a surface chemical reaction can give rise to different convective regimes. The physical system under analysis is a rigid cavity whose boundaries do not allow flow through. One of the boundaries will be considered to catalyze a chemical reaction and the opposite will be assumed to be permeable to reactants and product diffusion while kept at a constant temperature. The remaining two sides are rigid walls, while the whole cavity is considered perfectly thermally insulated (adiabatic).

To simplify the analysis of this problem it will be assumed here that a two-dimensional description will suffice. Even though in finite domains it is not strictly true that two-dimensional convective structures will prevail rather than three-dimensional ones, such an hypothesis is made here. With such a purpose, an infinite rectangular duct is studied. Thus it can be assumed that the influence of the rear and front walls is negligible for the problem analyzed here, and in a narrow region inside the system the two-dimensional description will be satisfactory. In the case of a duct of finite length, a similar analysis could be performed if only Davis' "rolls" were considered (see Davis[20]).

Under these assumptions the heat and mass transfer processes will be governed by the following dimensionless equations:

$$\frac{\partial y}{\partial t} = -\mathbf{u}\cdot\nabla y + \mathrm{Le}\,\nabla^2 y, \tag{1}$$

$$\frac{\partial \theta}{\partial t} = -\mathbf{u}\cdot\nabla\theta + \nabla^2\theta, \tag{2}$$

subject to

$$\frac{\partial y}{\partial x}=\frac{\partial \theta}{\partial x}=0\,, \quad \text{at } x=0,1 \text{ for } 0\leqslant z\leqslant 1\,, \tag{3}$$

$$y=\theta=0\,, \quad \text{at } z=1 \text{ for } 0\leqslant x\leqslant 1\,, \tag{4}$$

$$B\,\mathrm{Le}\frac{\partial y}{\partial z}=\frac{\partial \theta}{\partial z}=-\mathrm{FK}\,R(y,\theta)\,,$$

$$\text{at } z=0 \text{ for } 0<x<1\,, \tag{5}$$

where y and θ indicate the dimensionless conversion and temperature, respectively; and x, z, and t are the dimensionless directions and time while $\mathbf{u}=(u_x,u_z)$ is the dimensionless velocity vector. The dimensionless numbers that appear are the Lewis number (Le), the adiabatic temperature rise (B), the Damkohler number (Da), and the Frank–Kamenetskii parameter ($\mathrm{FK}=B\,\mathrm{Da}$). Here $R(y,\theta)=(1-y)^n\exp[\theta/(1+\theta/\gamma)]$ indicates the rate of reaction expression for an nth-order irreversible chemical reaction, where γ is the dimensionless activation energy.

For the description of the flow field, the Boussinesq approximation is considered valid. The fluid density is considered constant everywhere except in the external forces term. The dimensionless velocity–vorticity formulation is

$$\frac{\partial \omega}{\partial t}=-\mathbf{u}\cdot\nabla\omega+\mathrm{Pr}\,\nabla^2\omega+\frac{\mathrm{Pr}}{\alpha}\left(\mathrm{Ra}_1\frac{\partial \theta}{\partial x}+\mathrm{Ra}_2\frac{\partial y}{\partial x}\right), \tag{6}$$

with

$$\omega=\nabla^2\psi \tag{7}$$

subject to

$$\psi=\mathbf{n}\cdot\nabla\psi=0\,, \quad \text{along the boundaries,} \tag{8}$$

where ω is the vorticity, ψ is the streamfunction such that

$$\mathrm{curl}\,\psi=\left(-\frac{\partial \psi}{\partial z},\frac{1}{\alpha}\frac{\partial \psi}{\partial x}\right)$$

is the velocity vector, α is the aspect ratio (width/height), and the dimensionless numbers are the Rayleigh number (Ra_1), the concentration analog Rayleigh number (Ra_2), and the Prandtl number (Pr). The definitions of the dimensionless parameters and variables are identical to those reported in the study of Pribytkova *et al.*[9]

Equations (1)–(8) are solved numerically using an explicit finite difference scheme with central differences for the second-order terms and first-order upwind for the convective terms. The mass and temperature boundary conditions are solved by using standard Newton–Raphson iteration, and the Poisson equation for the streamfunction is solved by using cyclic reduction as proposed by Sweet and Swarztrauber.[21]

III. PRELIMINARIES

In the basic state, the fluid is motionless ($\psi\equiv 0$) and conduction and diffusion are the only modes of heat and mass transfer. The basic state (θ_0, y_0) is described by

$$\mathrm{Le}\frac{d^2y_0}{dz^2}=0\,, \tag{9}$$

$$\frac{d^2\theta_0}{dz^2}=0\,, \tag{10}$$

with boundary conditions given by Eqs. (3)–(5). The solutions to Eqs. (9) and (10) are

$$y_0=\theta_m/(B\,\mathrm{Le})(1-z)\,, \tag{11}$$

$$\theta_0=\theta_m(1-z)\,, \tag{12}$$

where θ_m is the maximum temperature in the system achieved on the catalytic surface. This temperature is the solution of

$$\theta_m=\mathrm{FK}\,R\,[\theta_m/(\mathrm{B\,Le}),\theta_m]\,. \tag{13}$$

For irreversible kinetics of arbitrary order and by taking reactant depletion into consideration, Eq. (13) can have either one or three distinct positive roots (two is an exceptional case). The smallest root (θ_{m1}) is associated with a kinetic regime (the reaction temperature is low and the reaction proceeds slowly). The second root (θ_{m2}) is an unstable solution and the chemical reaction will either extinguish (going to the kinetic regime) or ignite (going to the diffusion regime). The largest root (θ_{m3}) is associated with the stable diffusion regime. The later operating mode is characterized by high temperatures, while a very fast chemical reaction is controlled by the diffusion of the reactants to the catalytic surface. In Fig. 1 the bifurcation diagram of Eq. (13) (θ_m,Da) is presented. The region of multiple solutions is bounded by $\mathrm{Da}_*\leqslant \mathrm{Da}<\mathrm{Da}^*$.

It should be stressed that, depending on the Damkohler number (Da), the basic states will differ and so will the results of the linear stability analysis that are strongly dependent on those basic states.

IV. LINEAR STABILITY ANALYSIS

As was done by Pribytkova *et al.*,[9] in the rest of this work the thermal Rayleigh number (Ra_1) will be the bifurcation parameter and the rest of the parameter set will remain constant.

Perturbing the basic state in the usual manner,

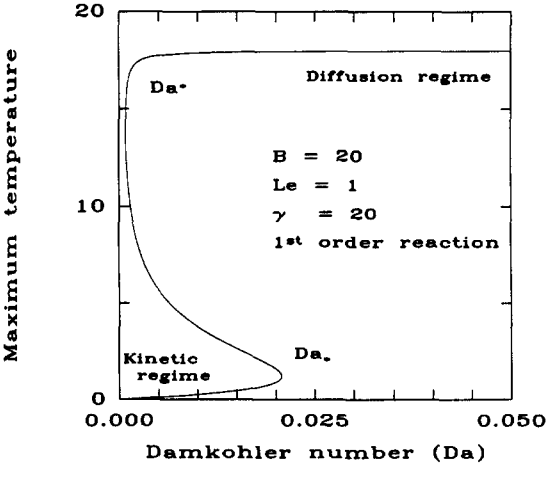

FIG. 1. Multiplicity of basic solutions.

$$y = y_0 + \epsilon y_1 + \epsilon^2 y_2 + \cdots,$$
$$\theta = \theta_0 + \epsilon\theta_1 + \epsilon^2\theta_2 + \cdots,$$
$$\psi = \psi_0 + \epsilon\psi_1 + \epsilon^2\psi_2 + \cdots,$$

with

$$\mathrm{Ra}_1 = \mathrm{Ra}_{1c} + \epsilon\,\mathrm{Ra}_1^1 + \epsilon^2\,\mathrm{Ra}_1^2 + \cdots$$

and substituting them into Eqs. (1), (2), and (6) yields

$$\frac{\partial y_1}{\partial t} = \mathrm{Le}\,\nabla^2 y_1 - \frac{1}{\alpha}\frac{\partial\psi_1}{\partial x}\frac{dy_0}{dz}, \tag{14}$$

$$\frac{\partial\theta_1}{\partial t} = \nabla^2\theta_1 - \frac{1}{\alpha}\frac{\partial\psi_1}{\partial x}\frac{d\theta_0}{dz}, \tag{15}$$

$$\frac{\partial}{\partial t}(\nabla^2\psi_1) = \mathrm{Pr}\,\nabla^4\psi_1 + \frac{\mathrm{Pr}}{\alpha}\left(\mathrm{Ra}_{1c}\frac{\partial\theta_1}{\partial x} + \mathrm{Ra}_2\frac{\partial y_1}{\partial x}\right). \tag{16}$$

The boundary conditions at $z = 0$ now take the form

$$\frac{\partial y_1}{\partial z} = -\frac{\mathrm{FK}}{B\,\mathrm{Le}}\left(\frac{\partial R}{\partial\theta}\theta_1 + \frac{\partial R}{\partial y}y_1\right), \tag{17}$$

$$\frac{\partial\theta_1}{\partial z} = -\mathrm{FK}\left(\frac{\partial R}{\partial\theta}\theta_1 + \frac{\partial R}{\partial y}y_1\right), \tag{18}$$

where, to make the problem more tractable, the reaction rate expression has been expanded in a Taylor series around the basic state (y_0,θ_0).

The solution (y_1,θ_1,ψ_1) of this eigenvalue problem will be sought in the following form:

$$y_1 = \sum_{k=1}^{N}\Upsilon_k(z)g_k(x)\exp(\sigma t), \tag{19}$$

$$\theta_1 = \sum_{k=1}^{N}\Theta_k(z)g_k(x)\exp(\sigma t), \tag{20}$$

$$\psi_1 = \sum_{k=1}^{N}\Psi_k(z)h_k(x)\exp(\sigma t), \tag{21}$$

where

$$g_k(x) = \exp\{i\pi/2k\,[\cos(\pi x) + 1]\},$$
$$h_k(x) = \exp(i\pi/2\{k\,[\cos(\pi x) + 1] - 1\}).$$

The choice of the horizontal perturbations is based on the fact that ψ must satisfy both Dirichlet and Neumann boundary conditions simultaneously. A Fourier series would be incorrect to use, since the lateral walls are not free surfaces.

The nonslip condition at the walls leads to slower velocities near the wall. This implies that convection is becoming less prominent and only conduction/diffusion are present. Furthermore, the lateral walls are adiabatic and impermeable, and no horizontal heat and mass flux occur. Thus only axial (vertical) diffusion processes will prevail near the walls and they will be described by the basic state. Hence it can be argued that for temperature and concentration perturbations, Neumann and Dirichlet boundary conditions will also hold at those walls. The nonslip and nonpenetration boundary conditions at the horizontal surfaces lead to a similar choice for $\Psi(z)$ as in the x direction, and $\Psi(z)$ becomes

$$\Psi_k(z) = S_k\sin\{\pi/2m[\cos(\pi z) + 1]\}.$$

Upon inspection of Eqs. (11) and (12), it is clear that the basic states of concentration and temperature differ only by a constant. For small disturbances to these states, it can be assumed that the spatial similarity between concentration and temperature will be preserved. Furthermore, Eq. (5) also shows that the boundary conditions at the catalytic surface differ by the same constant, and both perturbations satisfy Dirichlet boundary conditions at $z = 1$. Hence (Υ,Θ) will be sought in the following form:

$$\Upsilon_k(z) = Y_k f(z),$$
$$\Theta_k(z) = T_k f(z).$$

Upon substitution of these functions into Eqs. (17) and (18), and applying the Galerkin method in the x direction, the following eigenvalue problem results at $z = 0$:

$$Y_1\frac{df}{dz} = -\frac{\mathrm{FK}}{B\,\mathrm{Le}}\left(\frac{\partial R}{\partial\theta}T_1 f(0) + \frac{\partial R}{\partial y}Y_1 f(0)\right), \tag{22}$$

$$T_1\frac{df}{dz} = -\mathrm{FK}\left(\frac{\partial R}{\partial\theta}T_1 f(0) + \frac{\partial R}{\partial y}Y_1 f(0)\right). \tag{23}$$

Nontrivial solutions (Y_1,T_1,S_1) will only exist if

$$\frac{df}{dz}\frac{\mathrm{FK}}{B\,\mathrm{Le}}\frac{\partial R}{\partial y}f(0) + \left(\frac{df}{dz}\right)^2 + \mathrm{FK}\frac{\partial R}{\partial\theta}f(0)\frac{df}{dz} = 0. \tag{24}$$

At this point it is proper to introduce an explicit form of $R(y,\theta)$. If the kinetic is of the Arrhenius type, without loss of generality, the rate of reaction expression can be written as

$$R(y,\theta) = R_1(y)R_2(\theta).$$

One possible solution for Eq. (24) is

$$\frac{df}{dz} = 0;$$

this solution implies that

$$R_1(y)\frac{\partial R_2}{\partial\theta}T_1 f(0) + R_2(\theta)\frac{\partial R_1}{\partial y}Y_1 f(0) = 0.$$

If $f(0)\neq 0$, this solution will be valid only if

$$R_1(y)\frac{\partial R_2}{\partial\theta} = -\frac{Y_1}{T_1}R_2(\theta)\frac{\partial R_1}{\partial y},$$

which constitutes an exceptional combination of $(B,\mathrm{Da},\mathrm{Le})$. If $f(0) = 0$, it would imply that y_1 and θ_1 are identically zero. As mentioned before, it will be expected that diffusion processes dominate adjacent to the rigid surfaces. At the catalytic surface, adiabaticity and impermeability conditions are not present and it would be incorrect to use $df/dz = 0$, since the diffusion contribution of y_1 and θ_1 would be neglected.

Therefore, more general solutions of Eq. (24) will be sought. It has been assumed that y and θ (to first order) will only differ by a constant and hence $R_1(y)R_2(\theta) = R(\theta)$. Since $f(z)$ must meet the asymptotic conditions

$$\text{(I)}\quad \lim_{\partial R/\partial\theta\to 0}\left.\frac{df}{dz}\right|_{z=0} = 0,$$

and

$$\text{(II)}\quad \lim_{\partial R/\partial\theta\to\infty} f(0) = 0,$$

a suitable choice for $f(z)$ is

$$f(z) = \sin[\pi(1-b)z + \pi b],$$

where $b \to \frac{1}{2}$ in case (I), and $b \to 0$ in case (II) [for $b = 1$, $f(z)$ would be trivial]. Substituting this choice of $f(z)$ into Eq. (24) gives

$$H(b) = \pi(1-b)\cos(\pi b)G(b) = 0\,, \tag{25}$$

where

$$G(b) = \left(\frac{\mathrm{FK}}{B\,\mathrm{Le}}\frac{\partial R}{\partial y}\sin(\pi b) + \pi(1-b)\cos(\pi b) + B\,\mathrm{Da}\frac{\partial R}{\partial \theta}\sin(\pi b)\right).$$

When $b = 1$, $f(z)$ is trivial, and when $b = 2n - 1$, $n = 1,2,...$, it implies $df/dz = 0$, a case that was discussed earlier. This is illustrated in the following figures. In Fig. 2(a) the bifurcation diagram of the basic state is presented for a typical set of parameter values; it can be clearly seen that two different regimes are possible depending on the value of the Damkohler number. In Fig. 2(b), $G(b)$ is presented for a small value of the Damkohler number (kinetic regime) and a larger one (diffusion regime) in the range $0 \leqslant b \leqslant 1$. It follows that for small values of Da the right-hand side of Eqs. (22) and (23) are positive (for $B > 0$) and $\frac{1}{2} < b < 1$ is the proper root. For large values of Da, $df/dz > 0$ is possible and the root will be such that $0 < b < \frac{1}{2}$.

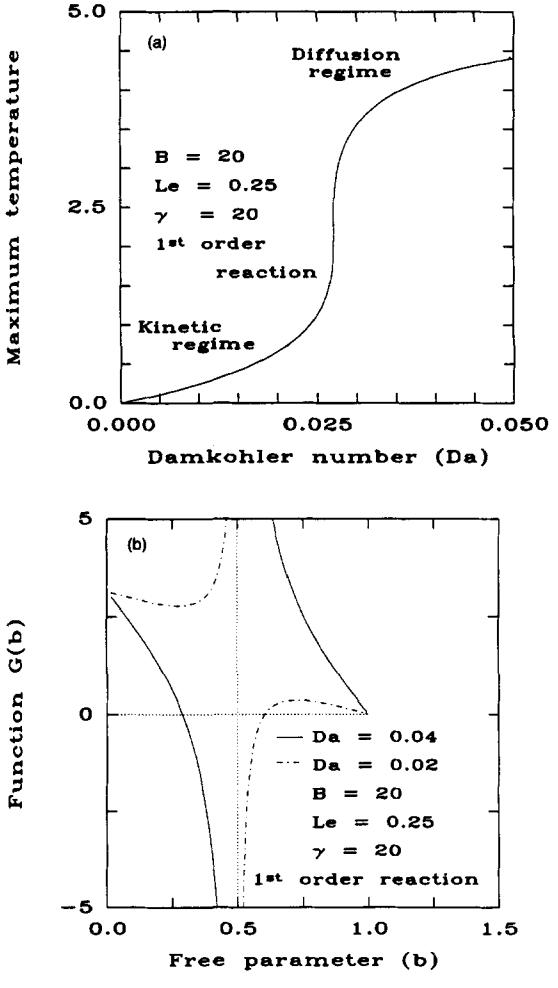

FIG. 2. Basic solutions for the reacting system. (a) Bifurcation diagram for the basic solution. (b) Solution for the trial function.

Returning to Eqs. (14)–(16) and applying the Galerkin method for these trial functions, the following set of ordinary differential equations is obtained (see also Appendix A):

$$L(\mu) = (\sigma_r + i\sigma_i)\mathrm{B}\mu\,, \tag{26}$$

where $\mu = [\mathbf{Y},\mathbf{T},\mathbf{S}]^T$, $\mathbf{Y} = [Y_1,...,Y_L,...,Y_N]^T$, $\mathbf{T} = [T_1,...,T_i,...,T_N]^T$, $\mathbf{S} = [S_1,...,S_i,...,S_N]^T$, and $L(\ )$ is a linear operator that maps elements of C^{3N} into itself. This is an N-mode truncation of (y_1,θ_1,ψ_1). It is important to note that the different modes are not necessarily independent (i.e., B in general will not be a diagonal matrix). For monotonic exchange of stabilities the complex number σ_i is zero. Many combinations of the system parameters have been investigated and the results can be summarized as follows. If the mass diffusivity equals the thermal diffusivity, oscillatory convection cannot be found. For Le = 1 the concentration field follows the temperature evolution. The energy and mass balances can be reduced to the equation for the invariant $(y - \theta/B)$ with the Dirichlet boundary condition at the top of the system ($z = 1$) and Neumann boundary condition at the catalytic surface ($z = 0$). Both Rayleigh numbers can be also grouped as $\mathrm{Ra} = \mathrm{Ra}_1 + \mathrm{Ra}_2/B$, and the principle of exchange of stabilities holds. However, for $\mathrm{Le} < 1$ and $\mathrm{Ra}_1 \times \mathrm{Ra}_2 < 0$, the first exchange of stabilities can occur for $\sigma_i \neq 0$ and the onset of oscillatory convection can be observed. This can be illustrated for two typical sets of the parameter values. Thus in Fig. 3(a) the neutral stability curve is shown for Le = 1, Da = 0.04 (diffusion regime), Pr = 0.7, $B = 8$, $\gamma = 20$, and $\mathrm{Ra}_2 = -5000$. In Fig. 3(b) the moduli for the corresponding eigenvalues are presented. The fact that the eigenvalues vanish indicates that the curve in Fig. 3(a) corresponds to the onset of monotonic instabilities. In Fig. 4(a), all conditions have been kept identical with the exception of the Lewis number, which is Le = 0.25; for those conditions the curve in Fig. 4(a) marks the onset of oscillatory convection as indicated by the corresponding eigenvalues presented in Fig. 4(b) whose imaginary parts do not cancel. To obtain both figures, the truncation point was $N = 6$; as α increases, more modes need to be considered and the computational effort increases drastically. These low truncation methods, especially for dependent modes, involve some trial and error. Usually the order of truncation is increased until the changes in the critical values become negligible.

To study the behavior of the system beyond criticality, it is necessary to extend the analysis by retaining the nonlinear terms. By taking the nonlinear convection terms into consideration, Bdzil and Frisch[5] did a nonlinear study of the Bénard case with a homogeneous reaction superimposed on it. In the next section a nonlinear analysis, based on the interaction of different modes,[22] is presented.

V. NONLINEAR STABILITY ANALYSIS

In a confined cavity only a finite number of modes will be stabilized and it could be argued that only the participating modes need to be considered. Although it is a heuristic argument, an inspection of Fig. 3 supports this claim. For

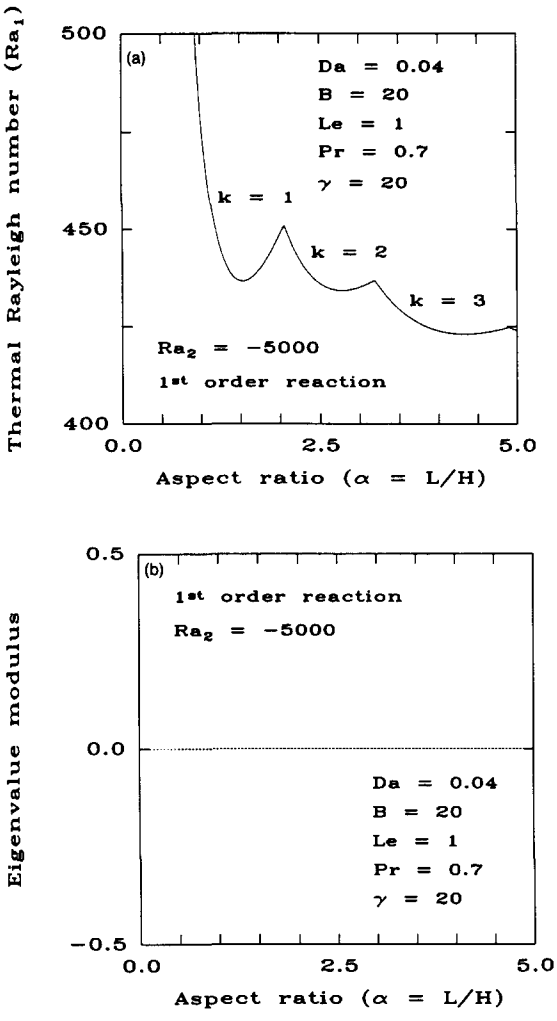

FIG. 3. Stability limits for the onset of monotonic instabilities. (a) Neutral stability curve. (b) Moduli of the corresponding eigenvalues.

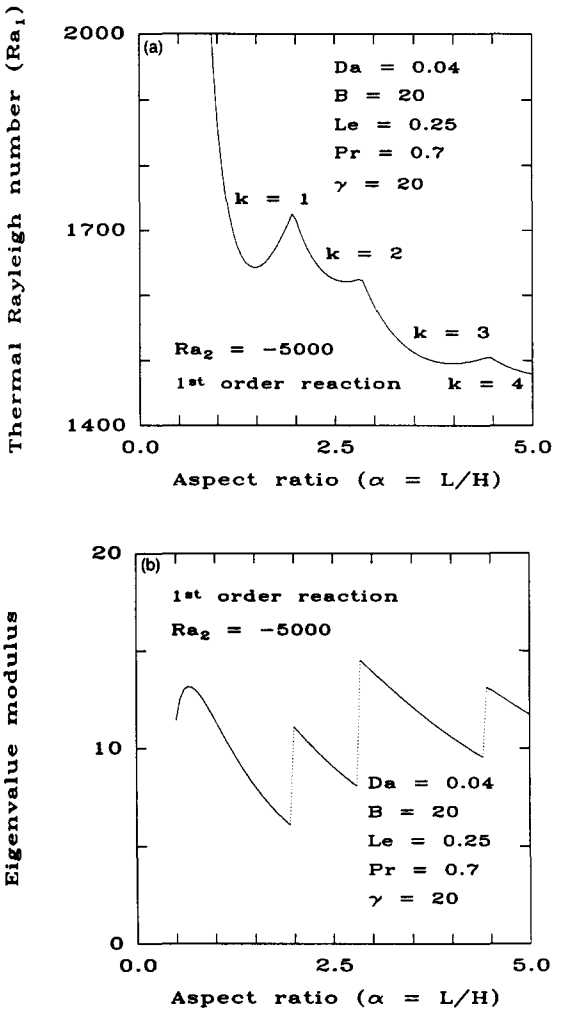

FIG. 4. Stability limits for the onset of oscillatory instabilities. (a) Neutral stability curve. (b) Moduli of the corresponding eigenvalues.

instance, when $\alpha = 2$ the system will experience one- and two-cell interactions and these cells will be affected by the third and fourth modes, respectively. The neutral curve at $\alpha = 2$ constitutes a two-vortex solution and the role of $k = 4$ is merely to modulate the two cells. When the Rayleigh number exceeds the critical value (Ra_{1c}), the first interaction will be with the neighboring first and third modes. In this work it is assumed that the conduction/diffusion basic states remain unchanged when convection develops and the latter mode is merely superimposed on the basic state. These arguments lead to the following ansatz:

$$y_{\mathrm{CV}} = f(z) \sum_{k=1}^{N} Y_k(t) g_k(x) ,$$

$$\theta_{\mathrm{CV}} = f(z) \sum_{k=1}^{N} T_k(t) g_k(x) ,$$

$$\psi_{\mathrm{CV}} = \sum_{m=1}^{M} h_m(z) \sum_{k=1}^{N} S_k(t) h_k(x) ,$$

where

$$(y,\theta,\psi) = \boldsymbol{\mu} = \boldsymbol{\mu}_0(z) + \boldsymbol{\mu}_{\mathrm{CV}}(x,z,t) .$$

In the rest of this study the number of modes in the z direction (M) will be considered as one (i.e., $M = 1$). The function $f(z)$ takes the same form as in the linear analysis. Since this function only depends on Da, B, Le, γ, and the order of reaction, it is invariant to the bifurcation parameter Ra_1. The same values for the parameter set as described in Fig. 3 will be used.

The aspect ratio (α) plays a very important role and $\alpha = 2$ and $\alpha = 4$ will be considered with truncations of $N = 3$ and $N = 6$, respectively. Substituting for these trial functions into Eqs. (1)–(7) and applying the Galerkin method, a set of ordinary differential equations results. This set can be written as (see Appendix B for details)

$$\dot{\boldsymbol{\mu}}_{\mathrm{CV}} = P(\boldsymbol{\mu}_{\mathrm{CV}}, \mathrm{Ra}_1, \alpha) , \tag{27}$$

and for fixed α, a bifurcation diagram $\|\boldsymbol{\mu}_{\mathrm{CV}}\|$ vs Ra_1 can be constructed. In Figs. 5 and 6 the bifurcation diagrams are shown for $\alpha = 2$ and $\alpha = 4$, respectively. For $\alpha = 2$ the system becomes unstable at Ra_{1L} and a limit cycle appears. The periodic branch is stable and the amplitude of the oscillations increases (in the L_2 sense) with increasing values of the thermal Rayleigh number. The critical value where the basic state becomes unstable, calculated by using Eq. (27), is

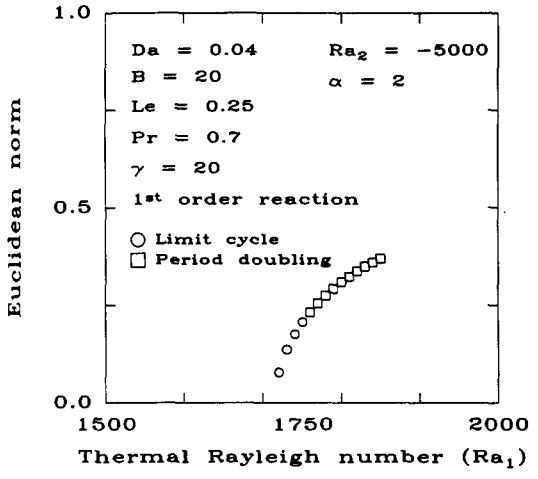

FIG. 5. Bifurcation diagram for $\alpha = 2$.

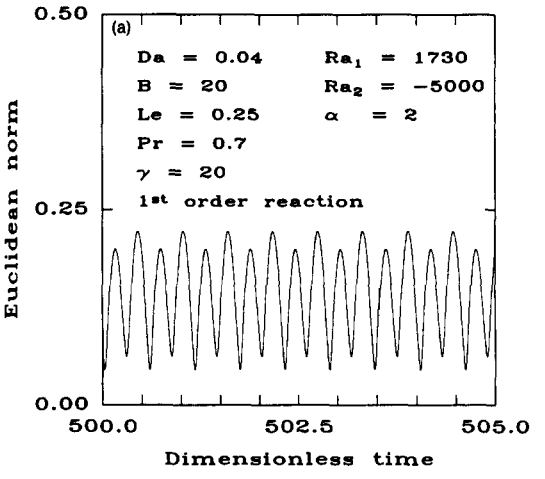

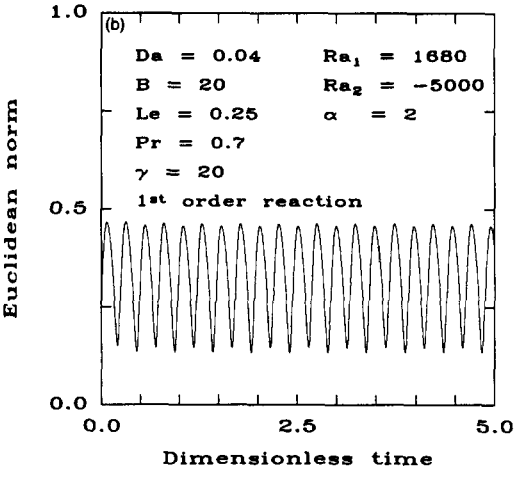

FIG. 7. Periodic behavior for $\alpha = 2$. (a) Nonlinear analysis. (b) Numerical results.

slightly larger than the numerical result. (It is known that the Galerkin method provides higher estimates.) The results are then compared in a qualitative sense and the values for the numerical verification are taken slightly lower than those predicted by the nonlinear analysis.

Figure 7 shows two time series. Figure 7(a) is a plot of the solution of Eq. (27) for $\alpha = 2$ and $\mathrm{Ra}_1 = 1730$, and Fig. 7(b) shows a plot of the numerical solution of Eqs. (1)–(8) for $\mathrm{Ra}_1 = 1680$. It clearly shows that the nonlinear analysis predicts the behavior of the model satisfactorily. Several points on the bifurcation diagram were numerically verified.

The bifurcation diagram presented in Fig. 6 shows an increasingly complex dynamic behavior. The conduction/diffusion basic state becomes unstable at Ra_{1L} and a limit cycle appears. This 1-p periodic branch bifurcates at Ra_{1P} and a 2-p limit cycle appears. For $\mathrm{Ra}_1 > \mathrm{Ra}_{1N}$ the time series shows chaotic behavior. In Fig. 8 the numerical results over one period of the limit cycle are presented. The series of contour plots shown in Figs. 9(a)–9(e) correspond sequentially to the points marked in Fig. 9. Over one period the four cells change their rotations and this occurs via an unstable six-mode route. In the contour plots shown the solid and dashed lines indicate clockwise and counterclockwise rotations, respectively.

The results of the numerical study are compared with

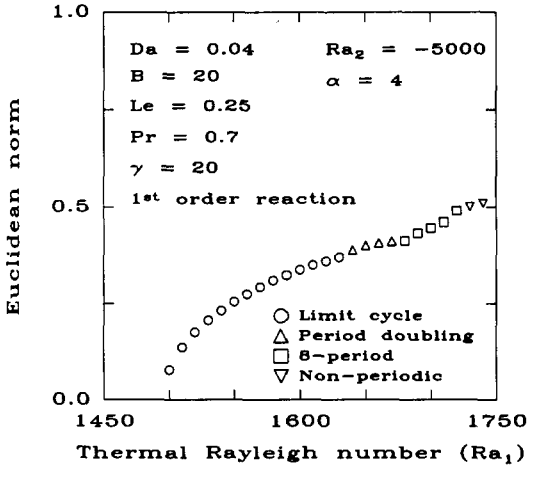

FIG. 6. Bifurcation diagram for $\alpha = 4$.

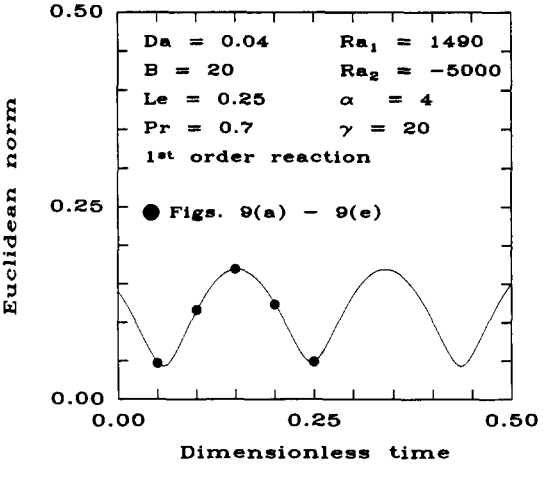

FIG. 8. Limit cycle for $\alpha = 4$.

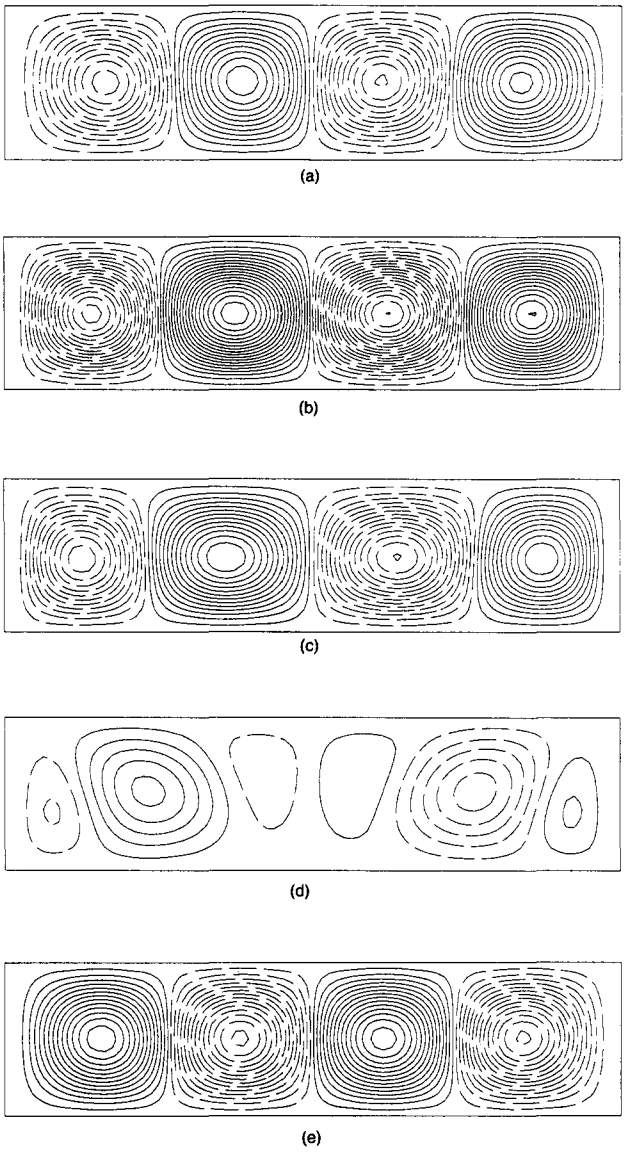

FIG. 9. Flow fields corresponding to Fig. 8.

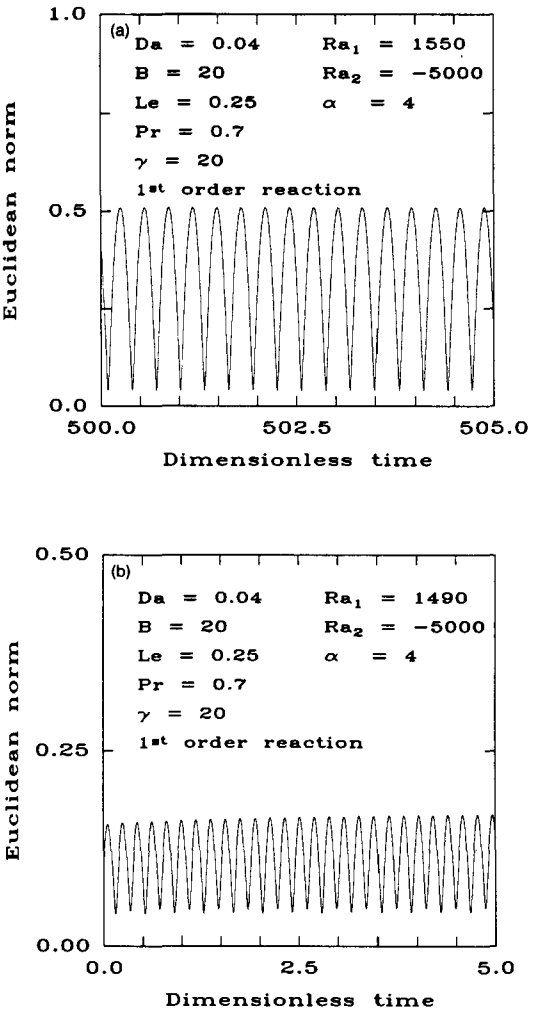

FIG. 10. Periodic behavior $\alpha = 4$. (a) Nonlinear analysis. (b) Numerical results.

the nonlinear analysis in Figs. 10–12. In Figs. 10(a) and 10(b) the time series for the nonlinear and numerical results are shown for $Ra_1 = 1550$ and $Ra_1 = 1490$, respectively. In Figs. 11(a) and 11(b) the results are shown for $Ra_1 = 1650$ and $Ra_1 = 1600$, respectively. In Figs. 12(a) and 12(b), $Ra_1 = 1750$ and $Ra_1 = 1700$ were used. Both series show chaotic behavior. This chaotic behavior is characterized by a strong competition between the different convective modes. Even though more than six modes were never observed numerically, the fluctuation between the different modes appears on a random basis.

In comparing the sets of Figs. 7(a), 10(a)–12(a) with the Figs. 7(b), 10(b)–12(b), similarities and discrepancies can be observed. In the derivation of the spectral equations higher harmonics have been neglected and this is a plausible explanation for the differences between the predictions of Eq. (27) and the numerical results. It is granted that the different values in the Ra_1 can give rise to further discrepancies. However, there is a striking qualitative similarity that suggests that the dominant harmonics have been retained.

VI. SUMMARY AND CONCLUSIONS

An analysis of convective instabilities in confined reactive fluid media has been presented. The driving force for convection is the gradient in the fluid density, which depends linearly on the concentration and temperature. This gradient is a result of the existence of a heterogeneous chemical reaction on one of the cavity walls. A linear stability analysis is presented and conditions for the onset of both monotonic and oscillatory convective instabilities are reported. The characteristic of the boundary conditions in a finite domain makes it difficult to choose an orthogonal basis for the trial functions, and explicit dispersion relations cannot be derived. In general, the conditions for the onset of oscillatory convective instabilities are disparity between mass diffusion and heat conduction (i.e., Lewis number different from unity) and opposite effects of the concentration and temperature on the fluid density (i.e., the thermal Rayleigh number and its analog mass Rayleigh number must have different signs). Such conditions can be observed in

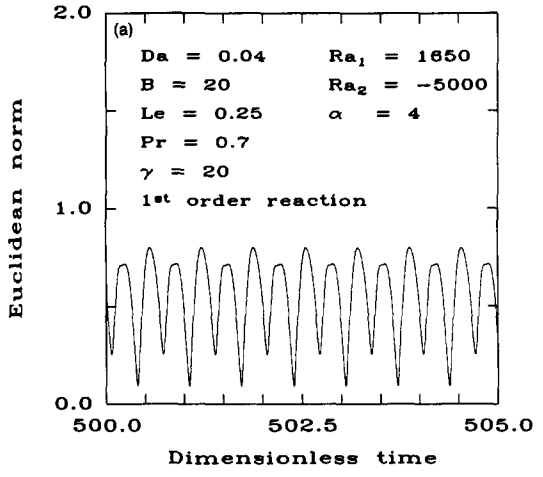

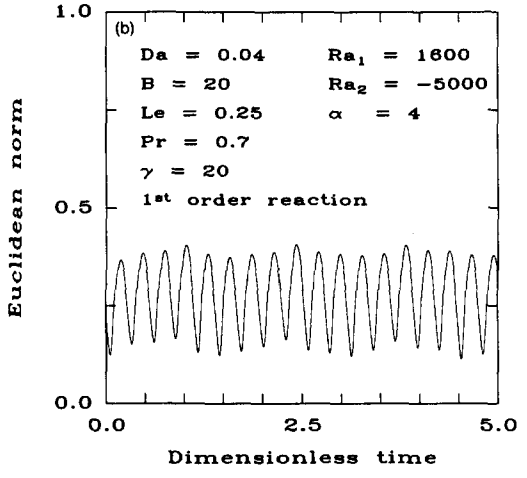

FIG. 11. Periodic behavior for $\alpha = 4$. (a) Nonlinear analysis. (b) Numerical results.

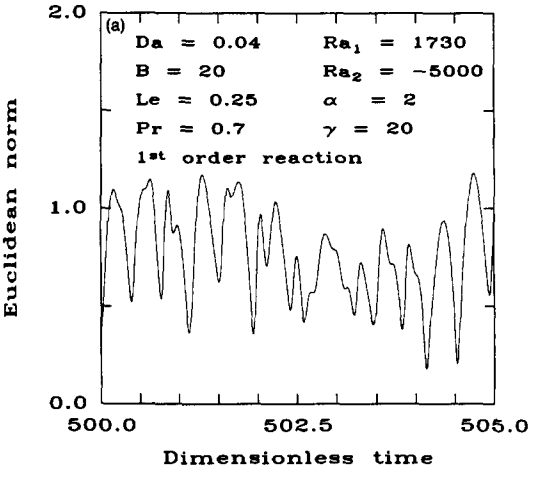

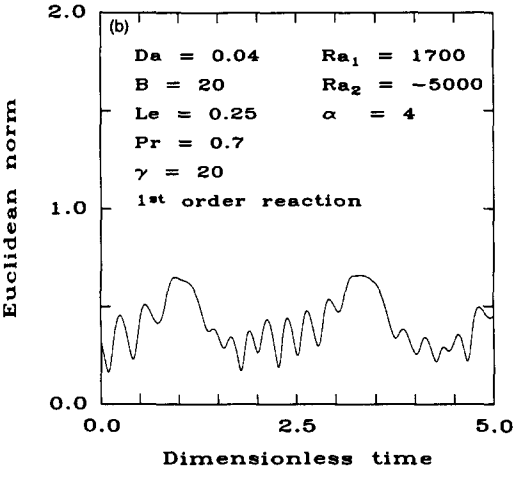

FIG. 12. Nonperiodic behavior for $\alpha = 4$. (a) Nonlinear analysis. (b) Numerical results.

many chemically reacting systems, for instance, endothermic reactions where a heavy product is formed at the warmer boundary. Based on the linear stability analysis an N-mode truncation is proposed. The stability of the convective modes is then studied by nonlinear stability analysis. It is shown how the dimension of the system is of great influence on the characteristic of periodic motions and very intricate flow patterns can be observed. As the systems becomes larger nonperiodic motion is the result. Numerical results of the original problem were provided and the stability predictions were confirmed.

The major goal of the presented analysis has been to understand new phenomena caused by the occurrence of convective instabilities. Since the problem without convective regimes is well understood, our strategy was to generalize this analysis for convective instabilities. This led us to a set of dimensionless criteria generally used in the literature. The results were reported for the parameter space of these dimensionless criteria, and certain cuts through the parameter space were presented. If parametric experiments were performed then a given dependence would be followed (e.g., dependence on the temperature at the top of the cavity). As pointed out by one of the reviewers, since an experimental path would not generally follow the typical crosscuts presented in this paper, the experimental points would define a trajectory that would occur on different intersections. Therefore, to follow an experimental path by theoretical calculations it is suggested that the analysis be performed by varying more than one parameter at a time. Thus, for a given reaction, the width and height of the system together with the temperature and reactant concentration at the top of the cavity can be identified as the main operating variables. Experiments conducted modifying the system width would alter the aspect ratio (α) only. This would provide data to verify stability predictions such as those presented in Figs. 3 and 4. On the other hand, changes in the system height (H) unfortunately would imply that more than one parameter would be modified (α, Ra_1, and Ra_2 would vary simultaneously) and in order to compare these experiments with theoretical predictions the latter ones should be performed in the corresponding parametric space. Identical comments can be made regarding experiments involving changes in the

temperature (Da, B, γ, and Ra_1 would vary simultaneously) or reactant concentration (Da, B, and Ra_2 would vary simultaneously) at the top of the cavity.

ACKNOWLEDGMENTS

The authors acknowledge the NCSA at the University of Illinois at Urbana–Champaign where the numerical computations were performed on a CRAY X-MP Supercomputer. The authors also want to thank the referees for their useful comments and suggestions.

Part of this work was supported by the National Science Foundation (NSF Grant No. CBT 86-10850); this support is gratefully acknowledged. Hendrik J. Viljoen acknowledges financial support of the National Research Institute for Mathematical Sciences, CSIR, South Africa. Jorge E. Gatica acknowledges partial financial support provided by a fellowship from the National Council for Scientific and Technological Research (CONICET) of the Republic of Argentina.

APPENDIX A: DERIVATION OF THE EIGENVALUE PROBLEM

The eigenvalue problem formulated in Eq. (26) is derived as follows. If the trial functions, as proposed by Eqs. (19)–(21), are replaced in the variational formulation of Eqs. (14)–(16), the following set of algebraic equations arises:

$$\sigma \mathsf{B}_Y \mathbf{Y} = \mathrm{Le}\, \mathsf{A}_Y^1 \mathbf{Y} + (1/\alpha)(\theta_m / B\,\mathrm{Le}) \mathsf{A}_Y^2 \mathbf{S}\,, \tag{A1}$$

$$\sigma \mathsf{B}_T \mathbf{T} = \mathsf{A}_T^1 \mathbf{T} + (1/\alpha)\theta_m \mathsf{A}_T^2 \mathbf{S}\,, \tag{A2}$$

$$\sigma \mathsf{B}_S \mathbf{T} = \mathrm{Pr}\, \mathsf{A}_S^1 \mathbf{S} + (\mathrm{Pr}/\alpha)(\mathrm{Ra}_1 \mathsf{A}_S^2 \mathbf{T} + \mathrm{Ra}_2 \mathsf{A}_S^3 \mathbf{Y})\,. \tag{A3}$$

If the Galerkin approach is used, the matrices are defined as

$$[\mathsf{B}_Y]_{ij} = [\mathsf{B}_T]_{ij} = \int\int_\Omega f^2(z) g_i(x) g_j(x)\, d\Omega\,,$$

$$[\mathsf{A}_Y^1]_{ij} = [\mathsf{A}_T^1]_{ij} = \int\int_\Omega f(z) g_i(x) \times \left(f''(z) g_j(x) + \frac{1}{\alpha^2} f(z) g_j''(x) \right) d\Omega\,,$$

$$[\mathsf{A}_Y^2]_{ij} = [\mathsf{A}_T^2]_{ij} = \int\int_\Omega f(z) g_i(x) h_1(z) h_j'(x)\, d\Omega\,,$$

$$[\mathsf{B}_S]_{ij} = \int\int_\Omega h_1(z) g_i(x) \left(h_1''(z) h_j(x) + \frac{1}{\alpha^2} h_1(z) h_j''(x) \right) d\Omega\,,$$

$$[\mathsf{A}_S^1]_{ij} = \int\int_\Omega f(z) h_1(z) h_i(x) g_j'(x)\, d\Omega\,,$$

$$[\mathsf{A}_S^2]_{ij} = [\mathsf{A}_S^3]_{ij} = \int\int_\Omega h_1(z) h_i(x) f(z) g_j'(x) d\Omega\,.$$

The system of Eqs. (A1)–(A3) can be rewritten as the following eigenvalue problem:

$$\mathsf{A}\boldsymbol{\mu} = \sigma \boldsymbol{\mu}\,, \tag{A4}$$

where

$$\boldsymbol{\mu} = [\mathbf{Y}, \mathbf{T}, \mathbf{S}]^T$$

and

$$\mathsf{A} = \begin{bmatrix} \mathrm{Le}\, \mathsf{B}_Y^{-1} \mathsf{A}_Y^1 & 0 & (1/\alpha)(\theta_m / B\,\mathrm{Le}) \mathsf{B}_Y^{-1} \mathsf{A}_Y^2 \\ 0 & \mathsf{B}_T^{-1} \mathsf{A}_T^1 & (\theta_m/\alpha) \mathsf{B}_T^{-1} \mathsf{A}_T^2 \\ \mathrm{Pr}\, \mathsf{B}_S^{-1} \mathsf{A}_S^1 & (\mathrm{Ra}_1/\alpha) \mathsf{B}_S^{-1} \mathsf{A}_S^2 & (\mathrm{Ra}_2/\alpha) \mathsf{B}_S^{-1} \mathsf{A}_S^3 \end{bmatrix}.$$

APPENDIX B: DERIVATION OF THE SPECTRAL EQUATIONS

If the trial functions proposed in Eqs. (19)–(21) are replaced in the variational formulation of the governing Eqs. (1)–(8) and the Galerkin approach is applied, the following ordinary differential equation system results:

$$\sum_{j=1}^N [\mathsf{B}_Y]_{ij} \dot{Y}_j = \mathrm{Le} \sum_{j=1}^N [\mathsf{A}_Y^1]_{ij} Y_j + \frac{1}{\alpha} \frac{\theta_m}{B\,\mathrm{Le}} \sum_{j=1}^N [\mathsf{A}_Y^2]_{ij} S_j + \frac{1}{\alpha} \sum_{j=1}^N \sum_{k=1}^N [\mathsf{A}_Y^3]_{ij,k} S_j Y_k\,, \tag{B1}$$

$$\sum_{j=1}^N [\mathsf{B}_T]_{ij} \dot{T}_j = \sum_{j=1}^N [\mathsf{A}_T^1]_{ij} T_j + \frac{1}{\alpha} \theta_m \sum_{j=1}^N [\mathsf{A}_T^2]_{ij} S_j + \frac{1}{\alpha} \sum_{j=1}^N \sum_{k=1}^N [\mathsf{A}_T^3]_{ij,k} S_j T_k\,, \tag{B2}$$

$$\sum_{j=1}^N [\mathsf{B}_S]_{ij} \dot{S}_j = \mathrm{Pr} \sum_{j=1}^N [\mathsf{A}_S^1]_{ij} S_j + \frac{\mathrm{Pr}}{\alpha} \left(\mathrm{Ra}_1 \sum_{j=1}^N [\mathsf{A}_S^2]_{ij} T_j + \mathrm{Ra}_2 \sum_{j=1}^N [\mathsf{A}_S^3]_{ij} Y_j \right) + \frac{1}{\alpha} \sum_{j=1}^N \sum_{k=1}^N [\mathsf{A}_S^4]_{ij,k} S_j S_k\,, \tag{B3}$$

where the matrices B_Y, B_T, B_S, A_Y^1, A_T^1, A_S^1, A_Y^2, A_T^2, A_S^2, and A_S^3 have the same meaning as in Appendix A, while

$$[\mathsf{A}_Y^3]_{i,j,k} = [\mathsf{A}_T^3]_{i,j,k} = \int\int_\Omega h_1'(z) f^2(z) g_i(x) h_j(x) g_k'(x) d\Omega - \int\int_\Omega h_1(z) f'(z) f(z) g_i(x) h_j'(x) g_k(x) d\Omega ,$$

$$[\mathsf{A}_S^4]_{i,j,k} = \int\int_\Omega h_1'(z) h_1'(z) h_1''(z) h_i(x) h_j(x) h_k'(x) d\Omega + \frac{1}{\alpha^2}\int\int_\Omega h_1^2(z) h_1'(z) h_i(x) h_j(x) h_k'''(x) d\Omega - \int\int_\Omega h_1^2(z) h_1'''(z) h_i(x) h_j'(x) h_k(x) d\Omega + \frac{1}{\alpha^2}\int\int_\Omega h_1^2(z) h_1'(z) h_i(x) h_j'(x) h_k''(x) d\Omega .$$

Thus the study of the stability of the convective modes can be done by solving the initial value problem posed by Eqs. (B1)–(B3).

[1] P. Metzener, Phys. Fluids **29**, 1373 (1986).
[2] R. D. Benguria and M. C. Depassier, Phys. Fluids **30**, 1678 (1987).
[3] R. P. Davies-Jones, J. Fluid Mech. **44**, 695 (1970).
[4] M. Gitterman and V. Steinberg, Phys. Fluids **26**, 393 (1983).
[5] J. B. Bdzil and J. L. Frisch, J. Chem. Phys. **72**, 1875 (1980).
[6] W. G. Gray and M. D. Kostin, Chem. Eng. J. **6**, 157 (1973).
[7] W. G. Gray and M. D. Kostin, Chem. Eng. J. **8**, 1 (1974).
[8] K. V. Pribytkova and E. A. Shtessel, Inz.-Fiz. Z. **30**, 263 (1976).
[9] K. V. Pribytkova, S. I. Khudyaev, and E. A. Shtessel, Inz.-Fiz. Z. **34**, 818 (1978).
[10] P. C. Wankat and W. R. Schowalter, AIChE J. **17**, 1346 (1971).
[11] P. C. Wankat and W. R. Schowalter, AIChE J. **18**, 769 (1972).
[12] S. G. Chefanov and E. A. Shtessel, Inz.-Fiz. Z. **30**, 818 (1976).
[13] E. N. Lorenz, J. Atmos. Sci. **20**, 130 (1963).
[14] J. H. Curry, Commun. Math. Phys. **60**, 193 (1978).
[15] C. Foias, O. P. Manley, and R. Temam, Phys. Fluids **29**, 3101 (1986).
[16] J. K. Platten and J. C. Legros, *Convection in Fluids* (Springer, Berlin, 1983), pp. 380–406.
[17] J. M. Luijkx and J. K. Platten, J. Non-Equilib. Thermodyn. **6**, 141 (1981).
[18] F. H. Busse, in *Transition and Turbulence*, edited by R. E. Meyer (Academic, New York, 1981), p. 43.
[19] H. J. Viljoen and V. Hlavacek, AIChE J. **33**, 1344 (1987).
[20] S. H. Davis, J. Fluid Mech. **30**, 465 (1967).
[21] P. N. Swarztrauber and R. A. Sweet, SIAM J. Numer. Anal. **5**, 900 (1977).
[22] G. Z. Gershuni and E. M. Zhukovitskii, *Convective Stability of Incompressible Fluids* (Keter, Jerusalem, 1976), p. 117.